

Decadal and Centennial ENSO Variability: MTM-SVD

Samantha Stevenson¹, Baylor Fox-Kemper¹, and Markus Jochum²

¹ATOC/CIRES, University of Colorado at Boulder, Boulder, CO; samantha.stevenson@colorado.edu

²National Center for Atmospheric Research (NCAR), Boulder CO

The new parameterization for atmospheric convection has greatly improved the representation of ENSO in the CCSM, but exactly what dynamical changes have resulted remains unclear. In an effort to diagnose these changes, the multitaper method/singular value decomposition (MTM-SVD; Lees & Park, 1995) method has been applied to our model run. The periods of interest are 50 years in length, and have been selected because they differ in mean state only in terms of the NINO3 variance present; making "P_LO" and "P_HI" excellent test cases for the effects of dynamical changes on ENSO behavior. The MTM-SVD method has proved effective at diagnosing ENSO in the past (Mann and Lees, 1996), and appears quite helpful in this case as well. We see marked changes in the distribution of variance with frequency in P_HI vs. P_LO, as well as dynamical effects which may represent changes in the importance of delayed-oscillator type wave dynamics relative to recharge and discharge of heat from the equatorial Pacific.

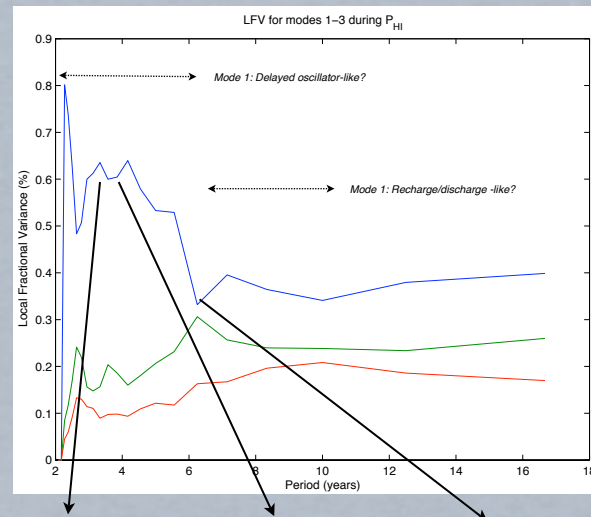
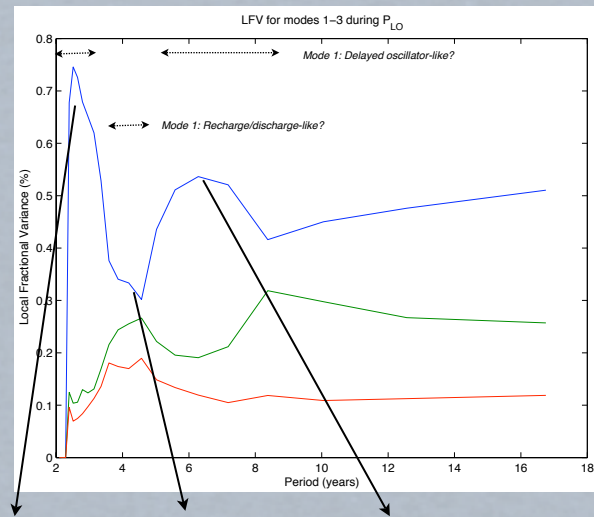
Periods of Interest

We have chosen two representative 50-year intervals in the 700-year CCSM3.5 run analyzed: P_HI and P_LO, so named for their NINO3 variances. Dynamics are vastly different in P_HI and P_LO!

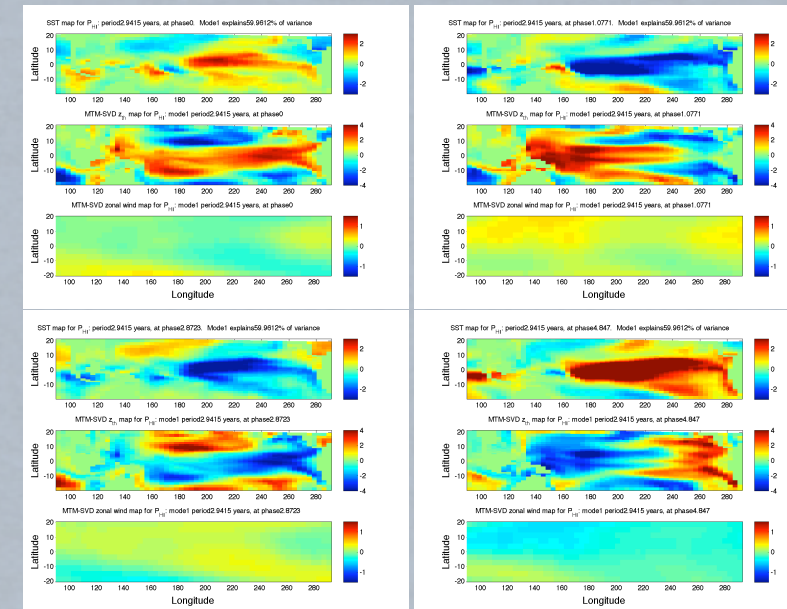
	Years	σ_{NINO3} (C^2)	Δz_{th} (m)	Mean z_{th} (m)	u (m/s)	σ_u (m^2/s^2)
P_LO	350-399	0.534	91.58	95.82	-14.64	0.517
P_HI	600-649	1.041	93.36	97.51	-14.86	0.528

Using MTM-SVD to Compare: P_LO vs. P_HI

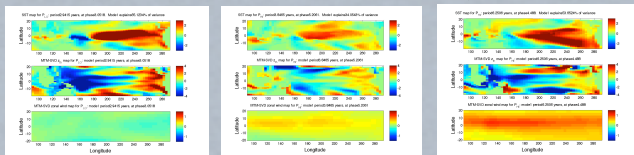
Local fractional variance (LFV) for P_LO (left) and P_HI (right), including the first three modes of the MTM-SVD.



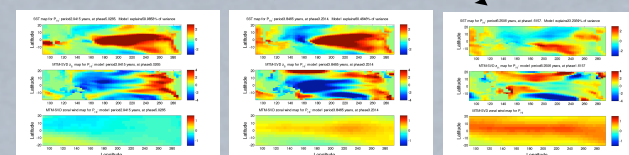
Example MTM-SVD Fields



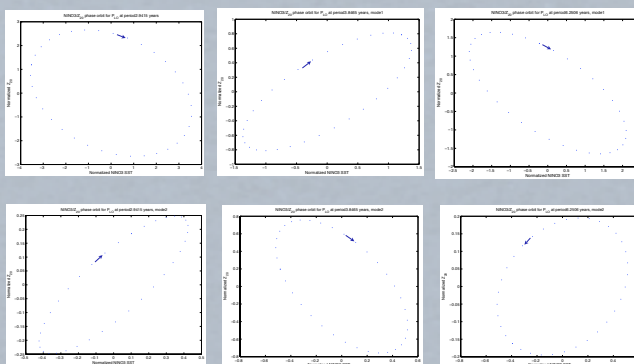
MTM-SVD decomposition during P_HI at an oscillation period of 2.94 years, in SST (top panels), thermocline depth (middle panels) and zonal wind (bottom panels). Four arbitrary phases are chosen for each, to illustrate the behavior of the oscillation in all fields.



P_LO: Maximum NINO3 amplitude MTM-SVD maps for the dominant mode of variability, at periods of 2.94, 3.84 and 6.25 years. ENSO-like variability in SST is apparent at 2.94 and 6.25 years, but at 3.84 an additional mode is present, possibly representing a recharge/discharge-like oscillation.



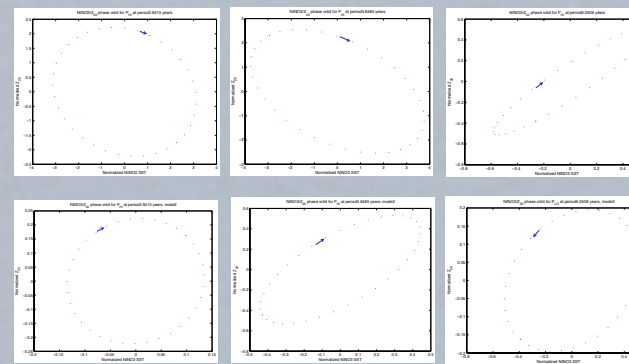
P_HI: Maximum NINO3 amplitude MTM-SVD maps for the dominant mode of variability, at periods of 2.94, 3.84 and 6.25 years. ENSO-like patterns in SST are visible, along with wave propagation in thermocline depth, for all periods less than 6 years. At this point, the dynamics appear to shift to a mode more governed by wind activity.



P_LO: Z20 (mean thermocline depth in the eastern Pacific (5S-5N, 130E-80W)) vs. NINO3 SST, following Kessler (2002). Plots shown for the dominant MTM-SVD mode (top) and second mode (bottom), at periods of 2.94, 3.84 and 6.25 years. Arrows indicate direction of increasing phase.

Mode 1

Mode 2



P_HI: Z20 (mean thermocline depth in the eastern Pacific (5S-5N, 130E-80W)) vs. NINO3 SST, following Kessler (2002). Plots shown for the dominant MTM-SVD mode (top) and second mode (bottom), at periods of 2.94, 3.84 and 6.25 years. Arrows indicate direction of increasing phase.

The application of the MTM-SVD decomposition method to data from a preliminary CCSM3.5 run has already yielded a great deal of information on the behavior of ENSO within the model. By comparing two 50-year segments of the run, it is possible to gain information on how precisely ENSO dynamics may differ within a single model, in the absence of other variations in the mean state.

Maps of MTM-SVD modes during P_HI and P_LO at various frequencies show that ENSO-like modes of variability appear and disappear as the period of oscillation changes. P_LO: Westward wave propagation is clearly visible in the first MTM-SVD mode (marked "delayed oscillator-like" in Figure 1), while at other times wave propagation is nearly absent. During times marked "recharge/discharge-like", zonal wind variability is dominated by basin-wide anomalies, which we hypothesize to lead to discharge of water from the equatorial Pacific via Sverdrup transport.

The transition from a wave-dominated oscillation to a wind-dominated oscillation in the first MTM-SVD mode occurs at different periods in P_LO vs. P_HI. In P_LO, the transition happens first at roughly 3 years, then wave activity resumes at 5 year periods. In P_HI, the dynamics appear much different: "delayed oscillator-like" variability persists until periods of 6 years, then disappear in favor of variability dominated by basin-wide wind anomalies.

We theorize that the marked difference in NINO3 variance in P_LO vs. P_HI, despite similarities in mean state between the two time periods, is a result of differences in interaction between distinct dynamical modes. Some modes are likely to resemble the "delayed oscillator", while others do not; these may be acting as "recharge/discharge" oscillators, or perhaps other dynamics come into play. Further work is necessary to diagnose the precise dynamical mechanisms at work throughout the model run.